PHYSICAL REVIEW D **82,** 037502 (2010)

Effect of η-η' mixing on $D \to PV$ decays

Bhubanjyoti Bhattacharya* and Jonathan L. Rosner†

Enrico Fermi Institute and Department of Physics, University of Chicago, 5640 S. Ellis Avenue, Chicago, Illinois 60637, USA

(Received 9 July 2010; published 19 August 2010)

Charmed meson decays to a light pseudoscalar (P) and light vector (V) meson are analyzed taking account of η-η' mixing. A frequently-used octet-singlet mixing angle of 19.5° is compared with a value of 11.7° favored by a recent analysis of $D \to PP$ decays.

DOI: 10.1103/PhysRevD.82.037502 PACS numbers: 13.25.Ft, 11.30.Hv, 14.40.Lb

Decays of the charmed mesons D^0, D^+, and D_s^+ to a light pseudoscalar meson P and a light vector meson V were analyzed within the framework of flavor SU(3) in Refs. [1,2]. A frequently-used octet-singlet mixing angle between η and η' of $\theta_\eta = 19.5°$ was used in Ref. [1], while Ref. [2] used $\theta_\eta = 14.4°$ based on a recent KLOE analysis [3]. In a study of $D_{(s)} \to PP$ [4], a best fit to Cabibbo-favored decay rates was found for $\theta_\eta = 11.7°$. In the present paper we update fits to $D_{(s)} \to PV$ decays including two decay modes not considered in [1], and compare fits based on $\theta_\eta = 19.5°$ and 11.7°.

We review our notation [4]. The angle θ_η describing octet-singlet mixing between η and η' is defined by

$$\eta = -\eta_8 \cos\theta_\eta - \eta_1 \sin\theta_\eta, \quad \eta' = -\eta_8 \sin\theta_\eta + \eta_1 \cos\theta_\eta, \tag{1}$$

where

$$\eta_8 \equiv (u\bar{u} + d\bar{d} - 2s\bar{s})/\sqrt{6}, \quad \eta_1 \equiv (u\bar{u} + d\bar{d} + s\bar{s})/\sqrt{3}, \tag{2}$$

Our previous analysis of PV decays utilized $\theta_\eta = \arcsin(1/3) = 19.5°$, for which

$$\eta = (s\bar{s} - u\bar{u} - d\bar{d})/\sqrt{3}, \quad \eta' = (2s\bar{s} + u\bar{u} + d\bar{d})/\sqrt{6}. \tag{3}$$

We consider also $\theta_\eta = 11.7°$, for which an exact fit was found in Ref. [4] to Cabibbo-favored decays.

We refer to Ref. [1] for notation. Amplitudes defined there include color-favored tree (T), color-suppressed tree (C), exchange (E), and annihilation (A), with a subscript P or V denoting the meson containing the spectator quark. Fitting the Cabibbo-favored data quoted there, we found two solutions ("A" and "B"), distinguished by $|T_V| < |C_P|$ (A) and $|T_V| > |C_P|$ (B). Fits to singly-Cabibbo-suppressed data then favored solutions consistent with the set "A," which we shall consider from now on. In Table I we show the results of this fit.

We then fit amplitudes involving η and η', obtaining values for the amplitudes T_P, C_V, and E_V. These are compared for the two-most-favored solutions (denoted by A1 and A2) in Tables II and III. Predictions for the branching fraction $\mathcal{B}(D^0 \to \bar{K}^{*0}\eta')$, listed in the last columns of Tables II and III, differ slightly between solutions A1 and A2.

Here we use a line of thought different from the analysis of Ref. [1]. We now calculate global χ^2 values for fits to singly-Cabibbo-suppressed $D^0 \to PV$ decays for the solutions A1 and A2. We compare the χ^2 values for the fit with $\theta_\eta = 19.5°$ [including branching fractions $\mathcal{B}(D^0 \to \eta\omega) = (0.221 \pm 0.023)\%$ [5] and $\mathcal{B}(D^0 \to \eta\phi) = (1.4 \pm 0.5) \times 10^{-4}$ [6] omitted in the original article] with values for a fit to the same data with $\theta_\eta = 11.7°$. These results are shown in Tables IV and V, respectively.

We see that solution A1 is favored for both $\theta_\eta = 19.5°$ and $\theta_\eta = 11.7°$. The solution A2 is disfavored since its prediction for $\mathcal{B}(D^0 \to \eta\phi)$ is much higher than the experimental value in both cases. The same conclusion is reached in Ref. [2] for $\theta_\eta = 14.4°$. We will now disregard the A2 solution and only use the A1 solution for the rest of the analysis.

The next step is to use observed Cabibbo-favored decays to obtain the annihilation amplitudes A_P and A_V using the amplitudes for $D_s \to (\bar{K}^{*0}K^+, \bar{K}^0K^{*+}, \pi^+\omega)$ (as quoted in Table VI) and the A1 solutions. Since we use only 3 independent inputs to obtain 4 independent parameters (real and imaginary parts of A_P and A_V) instead of obtaining unique solutions, we obtain a zone of allowed parameter space. We first form a grid of $|A_P|$ and $|A_V|$ values, and for every point on this grid, use the amplitudes for $D_s \to (\bar{K}^{*0}K^+, \bar{K}^0K^{*+})$ to obtain the phases of A_P and A_V relative to T_V (assumed real, as previously.) Thus for every point on

TABLE I. Solution in Cabibbo-favored charmed meson decays to PV final states favored by fits [1] to singly-Cabibbo-favored decays.

PV amplitude	Magnitude (10^{-6})	Relative strong phase
T_V	3.95 ± 0.07	$\cdots$
C_P	4.88 ± 0.15	$\delta_{C_PT_V} = (-162 \pm 1)°$
E_P	2.94 ± 0.09	$\delta_{E_PT_V} = (-93 \pm 3)°$

*bhujyo@uchicago.edu
†rosner@hep.uchicago.edu

TABLE II. Solutions for T_P, C_V, and E_V amplitudes in Cabibbo-favored charmed meson decays to PV final states. Solutions A1 and A2 correspond to $|T_V| < |C_P|$. Here the η-η' mixing angle is $\theta_\eta = 19.5°$.

No.	PV ampl.	Magnitude (10^{-6})	Relative strong phase	$\mathcal{B}(D^0 \to \bar{K}^{*0}\eta')$ (10^{-4})
A1	T_P	7.46 ± 0.21	Assumed 0	
	C_V	3.46 ± 0.18	$\delta_{C_V T_V} = (172 \pm 3)°$	1.52 ± 0.22
	E_V	2.37 ± 0.19	$\delta_{E_V T_V} = (-110 \pm 4)°$	
A2	T_P	6.51 ± 0.23	Assumed 0	
	C_V	2.47 ± 0.22	$\delta_{C_V T_P} = (-174 \pm 4)°$	1.96 ± 0.23
	E_V	3.39 ± 0.16	$\delta_{E_V T_V} = (-96 \pm 3)°$	

TABLE III. Same as Table II but with $\theta_\eta = 11.7°$.

No.	PV ampl.	Magnitude (10^{-6})	Relative strong phase	$\mathcal{B}(D^0 \to \bar{K}^{*0}\eta')$ (10^{-4})
A1	T_P	7.69 ± 0.21	Assumed 0	
	C_V	4.05 ± 0.17	$\delta_{C_V T_V} = (162 \pm 4)°$	1.19 ± 0.12
	E_V	1.11 ± 0.22	$\delta_{E_V T_V} = (-130 \pm 10)°$	
A2	T_P	5.68 ± 0.23	Assumed 0	
	C_V	1.74 ± 0.23	$\delta_{C_V T_P} = (-162 \pm 6)°$	2.19 ± 0.16
	E_V	3.82 ± 0.15	$\delta_{C_V T_V} = (-87 \pm 3)^c$	

TABLE IV. Global χ^2 values for fits to singly-Cabibbo-suppressed $D^0 \to PV$ decays. Also included are the process that contribute the most to a high χ^2 value. Here we have taken $\theta_\eta = 19.5°$.

No.	Global	Worst processes (Highest $\Delta\chi^2$ values)			
	χ^2	Decay channel	$\mathcal{B}_{\rm th}(\%)$	$\mathcal{B}_{\rm expt}(\%)$	$\Delta\chi^2$
A1	55.9	$D^0 \to \eta\phi$	$(4.0 \pm 0.4) \times 10^{-2}$	$(1.4 \pm 0.5) \times 10^{-2}$	16.8
		$D^0 \to \eta\omega$	0.33 ± 0.02	0.221 ± 0.023	11.3
A2	82.4	$D^0 \to \eta\phi$	$(5.9 \pm 0.4) \times 10^{-2}$	$(1.4 \pm 0.5) \times 10^{-2}$	45.8
		$D^0 \to \pi^0\rho^0$	0.27 ± 0.02	0.373 ± 0.022	10.1

TABLE V. Same as Table IV but with $\theta_\eta = 11.7°$.

No.	Global	Worst processes (Highest $\Delta\chi^2$ values)			
	χ^2	Decay channel	$\mathcal{B}_{\rm th}(\%)$	$\mathcal{B}_{\rm expt}(\%)$	$\Delta\chi^2$
A1	35.8	$D^0 \to \pi^+\rho^-$	0.39 ± 0.03	0.497 ± 0.023	8.5
		$D^0 \to \eta\omega$	0.30 ± 0.02	0.221 ± 0.023	6.7
A2	131.4	$D^0 \to \eta\phi$	$(9.2 \pm 0.6) \times 10^{-2}$	$(1.4 \pm 0.5) \times 10^{-2}$	100.0
		$D^0 \to \pi^0\rho^0$	0.27 ± 0.02	0.373 ± 0.022	11.4

TABLE VI. Branching ratios [6] and invariant amplitudes for Cabibbo-favored decays of D_s used to obtain A_P and A_V. θ_η is the η-η' mixing angle. $\phi_1 = \arcsin(1/\sqrt{3}) = 35.3°$.

Meson	Decay mode	Representation	$\mathcal{B}$ [6] (%)	p^* (MeV)	$\lvert\mathcal{A}\rvert$ (10^{-6})
D_s^+	$\bar{K}^{*0}K^+$	$C_P + A_V$	3.9 ± 0.6	682.4	3.97 ± 0.31
	$\bar{K}^0 K^{*+}$	$C_V + A_P$	5.3 ± 1.2	683.2	4.61 ± 0.52
	$\pi^+\omega$	$\frac{1}{\sqrt{2}}(A_V + A_P)$	0.25 ± 0.09	821.8	0.76 ± 0.14
	$\rho^+\eta$	$T_P\cos(\theta_\eta + \phi_1) - \frac{A_P+A_V}{\sqrt{2}}\sin(\theta_\eta + \phi_1)$	13.0 ± 2.2	723.8	6.63 ± 0.56
	$\rho^+\eta'$	$T_P\sin(\theta_\eta + \phi_1) + \frac{A_P+A_V}{\sqrt{2}}\cos(\theta_\eta + \phi_1)$	12.2 ± 2.0	464.8	12.5 ± 1.0

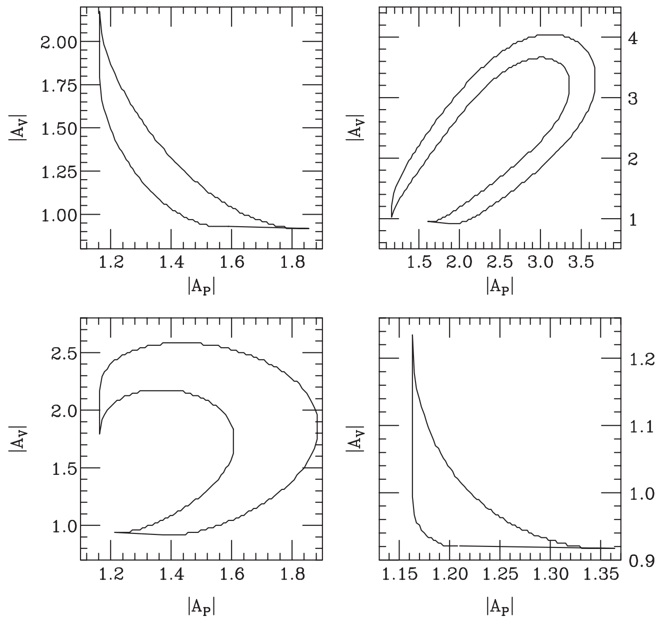

FIG. 1. Allowed values for $|A_P|$ and $|A_V|$ for $\theta_\eta = 19.5°$. In order to obtain the phase of $A_{P(V)}$ we either add (denoted by $+$) or subtract (denoted by $-$) its phase relative to $C_{V(P)}$ from the phase of $C_{V(P)}$. Clockwise from top left the 4 panels represent the phase choices: (a) $+\,+$, (b) $+\,-$, (c) $-\,-$, and (d) $-\,+$. Thus one may associate a unique value of the phase of $A_{P(V)}$ with every point on the parameter space in these plots.

this grid we now have an amplitude for the decay $D_s \to \pi^+\omega$ using the amplitude representation from Table VI. We now select only those points on this grid that are allowed by the experimental value $|\mathcal{A}(D_s \to \pi^+\omega)|$ including its one-sigma error bar.

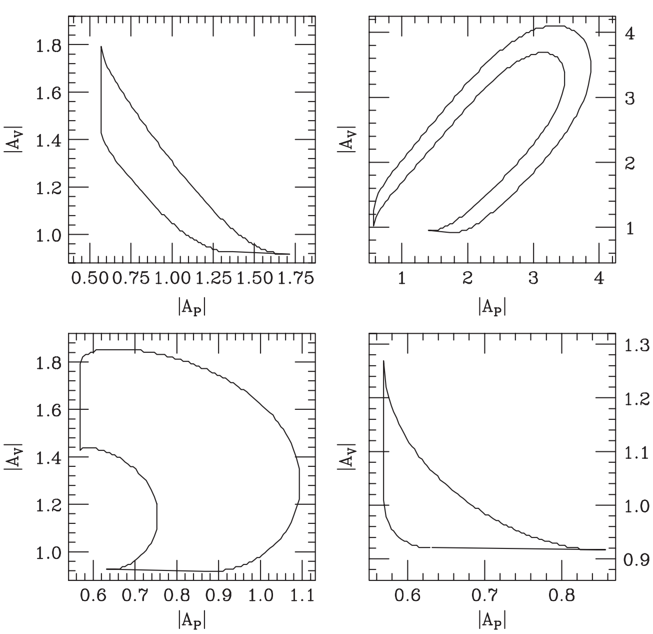

FIG. 2. Same as Fig. 1 but with $\theta_\eta = 11.7°$.

Since there is a twofold discrete ambiguity in choosing the phase of A_P relative to C_V or that of A_V relative to C_P, we obtain four different sets of allowed zones on the parameter space defined by $|A_P|$ and $|A_V|$. The allowed zones for $\theta_\eta = 19.5°$ and $\theta_\eta = 11.7°$ are shown in Figs. 1 and 2, respectively. One may associate unique phases with A_P and A_V (that may be determined following the method explained above) for every point on the $|A_P|$-$|A_V|$ plane in each of these figures.

To conclude one may now use the range of possible A_P and A_V values to predict $\mathcal{B}(D_s \to \eta\rho^+)$ and $\mathcal{B}(D_s \to \eta'\rho^+)$. In Ref. [1] we used the solution:

$$|A_P| = 1.36^{+1.16}_{-1.04}, \qquad \delta_{A_P} = (-151^{+83}_{-74})° \tag{4}$$

$$|A_V| = 1.25^{+0.34}_{-0.31}, \qquad \delta_{A_V} = (-19^{+10}_{-9})° \tag{5}$$

which led us to obtain $\mathcal{B}(D_s \to \eta\rho^+) = (5.6 \pm 1.2)\%$ and $\mathcal{B}(D_s \to \eta'\rho^+) = (2.9 \pm 1.2)\%$. Over the region of allowed values for $A_{P(V)}$, the central values for these Cabibbo-favored D_s branching ratios vary over the ranges shown in Table VII.

The predictions for $\mathcal{B}(D_s \to \eta\rho^+)$ are a bit higher in the new fit using $\theta_\eta = 11.7°$ and slightly closer to the experimental value [6] quoted in Table VI. No improvement is seen in the prediction for $\mathcal{B}(D_s \to \eta'\rho^+)$ in the new fit using $\theta_\eta = 11.7°$. The experimental values for both these branching ratios [6], as quoted in Table VI, are much higher than the predictions using this analysis. As mentioned in Ref. [1], the relation

$$|A(D_s \to \rho^+\eta')|^2 = |T_P|^2 + |A(D_s \to \pi^+\omega)|^2 - |A(D_s \to \rho^+\eta)|^2 \tag{6}$$

is very badly obeyed with the present values of $\mathcal{B}(D_s \to \eta\rho^+)$ and $\mathcal{B}(D_s \to \eta'\rho^+)$, leading us to suspect either that they have been overestimated experimentally, or that disconnected diagrams (as studied in [4]) play a larger role than anticipated. The scarcity of available data for Cabibbo-favored processes prevents such an analysis in the $D \to PV$ case.

This work was supported in part by the United States Department of Energy under Grant No. DE-FG02-90ER40560.

TABLE VII. Range of predicted branching ratios for $D_s \to (\eta, \eta')\rho^+$ using both $\theta_\eta = 19.5°$ and $\theta_\eta = 11.7°$.

Decay mode	$\theta_\eta = 19.5°$		$\theta_\eta = 11.7°$	
	Min(%)	Max(%)	Min(%)	Max(%)
$\mathcal{B}(D_s \to \eta\rho^+)$	3.80	6.39	6.27	8.35
$\mathcal{B}(D_s \to \eta'\rho^+)$	2.71	3.41	2.45	3.04

[1] B. Bhattacharya and J. L. Rosner, Phys. Rev. D **79**, 034016 (2009); Phys. Rev. D **81**, 099903 (2010).

[2] H.-Y. Cheng and C.-W. Chiang, Phys. Rev. D **81**, 074021 (2010).

[3] F. Ambrosino *et al.* (KLOE Collaboration), J. High Energy Phys. 07 (2009) 105.

[4] B. Bhattacharya and J. L. Rosner, Phys. Rev. D **81**, 014026 (2010).

[5] R. Kass (*BABAR* Collaboration) EPS2009, Krakow, Poland, http://pos.sissa.it/cgi-bin/reader/conf.cgi?confid=84.

[6] C. Amsler *et al.* (Particle Data Group), Phys. Lett. B **667**, 1 (2008), and partial 2009 update for the 2010 edition of Review of Particle Physics.